An X-Band Self-Mixing Oscillator Antenna for Transceiver and Spatial Power-Combining Applications

Claudio M. Montiel, *Member, IEEE*, Lu Fan, *Member, IEEE*, and Kai Chang, *Fellow, IEEE*

***Abstract*—The general theory for oscillator and mixer design is applied to develop an X-band self-mixing oscillator antenna. The antenna uses a Gunn diode as the active device that provides the oscillations and self-mixing operations. The circuit uses a slotline ring resonator for frequency stabilization and can be modified to include a varactor diode for wide-band frequency tuning. The circuit performance is compared with theoretical results derived from simple transmission-line models. The radiation patterns of the self-mixing oscillator antenna are also compared with those measured from a similarly configured passive antenna. Since the radiated power also serves as the local oscillator (LO) frequency for the self-mixing operation, the circuit is useful as a half-duplex transceiver. When the self-mixing operation is not required, a single oscillator antenna can be used as a transmitter and several units can be assembled in a planar array for spatial power-combining applications.**

***Index Terms*— Active antenna, power combining, self-mixing oscillator, transceiver.**

I. Introduction

OVER THE last few years, the direct integration of oscillator and amplifiers into antenna structures has received a great deal of attention because of the potential for reduced size, weight, and cost [1]–[3]. Self-mixing oscillators [4] and self-mixing active antennas [5] have also been demonstrated, but require careful analysis of the design tradeoffs involved.

The circuit presented in this paper offers many advantages. The circuit is extremely simple, requiring only one Gunn diode for oscillator and self-mixer operations. Thus, only one power supply is required for the basic circuit operation. In addition, the circuit is etched using photolithographic methods, which allow construction at a very low cost. The circuit does not require a metallized backplane for good performance. The incorporation of the slotline ring resonator and the slotline flared antenna result in excellent phase-noise stability and good radiation characteristics.

Manuscript received August 29, 1997; revised December 8, 1997. This work was supported in part by the U.S. Army Research Office, by the Texas Higher Education Coordinating Board's Advanced Technology Program, and by the U.S. Department of Education under a Fellowship for Research in Areas of National Need.

C. M. Montiel and L. Fan were with the Department of Electrical Engineering, Texas A&M University, College Station, Texas 77843-3128 USA. They are now with Texas Instruments Incorporated, Dallas, TX 75243-4136 USA.

K. Chang is with the Department of Electrical Engineering, Texas A&M University, College Station, TX 77843-3128 USA.

Publisher Item Identifier S 0018-9480(98)06727-1.

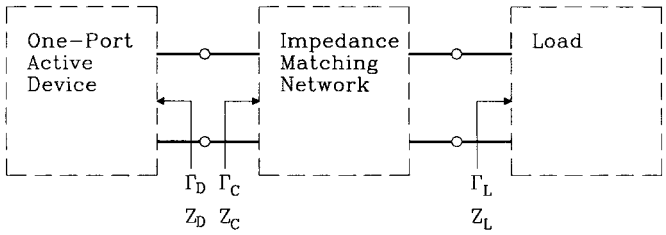

Fig. 1. Generalized one-port oscillator design. A GaAs Gunn diode is used as the active device for the oscillator active antenna. The load is a slotline flared antenna with exponential taper. The impedance-matching network consists of the Gunn diode's package parasitics and a slotline ring resonator.

II. Oscillator Antenna Design

Microwave oscillator design and microwave amplifier design are very closely related. In fact, the same transistors, dc-bias levels, and set of S-parameters can be used for oscillator and amplifier design. The circuit must be designed in such a way such that the load does not know whether it is connected to an oscillator or an amplifier. In the case of an active antenna, the load is the radiating structure itself.

The design of microwave oscillators is well understood and its general theory can be found in one of the many textbooks available, e.g., [6]–[8]. As such, a detailed development will not be given here; only a brief outline will be given and the results will be applied to the design at hand. There are two commonly used methods for the analysis and design of oscillators, depending on whether the active device is modeled as a one- or two-port network. This circuit uses a Gunn diode modeled as a one-port network.

Fig. 1 shows the generalized oscillator circuit for a one-port active device. The impedance of the active device can be expressed as

$$Z_D = -R_D + jX_D, \qquad \text{with} \quad R_D > 0. \tag{1}$$

The driving-point impedance seen by the diode is the impedance presented to the diode by the load and impedance-matching network. This driving-point impedance includes the diode package parasitic effects and embedding circuits. The circuit impedance can be expressed as

$$Z_C = R_C + jX_C. \tag{2}$$

The resonant frequency of the whole circuit determines the oscillating frequency. When the circuit is at resonance, the total reactance equals zero.

The conditions for oscillation start-up from noise require that

$$|\mathrm{Re}(Z_D)| - \mathrm{Re}(Z_C) \geq 0 \tag{3}$$

and

$$\mathrm{Im}(Z_D) + \mathrm{Im}(Z_C) = 0. \tag{4}$$

The oscillation will build up to steady-state condition and the negative resistance will decrease with increasing RF current until it is exactly equal to the circuit resistance (R_C) for this series circuit. There is a load circuit resistance, which produces optimum power. Typically, this optimum load resistance is about one-third of the small signal $-R_D$.

At the oscillating frequency f_o, the conditions for oscillation can be rewritten as

$$R_C(f_o) = R_D(f_o) \tag{5}$$

$$X_C(f_o) = -X_D(f_o). \tag{6}$$

The value of $R_D(f_o)$ in (5) will control the output power of the oscillator, while (6) will determine the oscillating frequency. In general, the device impedance is not only a function of frequency, but also depends on the dc-bias current, RF current generated, and operating temperature. Thus, (5) and (6) will also depend on these parameters.

III. Circuit Configuration and Modelling

The self-mixing oscillator antenna consists of a slotline notch antenna with a Gunn diode and a slotline ring resonator. The Gunn diode is placed across the slotline ring resonator at a low impedance point to meet the oscillation conditions given by (5) and (6). Since the Gunn diode is capable of oscillations over a range of frequencies and the slotline antenna is by nature a broad-band device, a slotline ring resonator is added to increase the frequency stability of the circuit. The slotline ring's resonant wavelength can be determined from

$$2\pi\overline{r} = n\lambda_g, \qquad \text{for } n = 1, 2, 3, \cdots \tag{7}$$

where $\overline{r}$ is the ring's mean radius, λ_g is the guide wavelength, and n is the mode number [9].

Fig. 2 shows the circuit configuration of the self-mixing oscillator antenna. The circuit was etched on a Duroid 5870 substrate, with a relative dielectric constant of 2.33, thickness of 62 mil (1.575 mm), and 1-oz copper metallization. The slotline ring resonator was designed for a characteristic impedance of 100 Ω and has a mean radius of 3.88 mm and a line width of 0.18 mm. The first resonant mode of the ring $(n = 1)$ occurs at 10 GHz for the dimensions given.

The slotline notch antenna uses an exponential taper to match the impedance of the ring to free space. The antenna length from the feedpoint to the end of the substrate is 60 mm. The gap at the feed point is 0.18 mm and the gap at the mouth of the antenna is 31.5 mm. The Gunn diode is mounted on a piece of aluminum that serves as the heat sink required by the low dc-to-RF conversion efficiency of the diode. The dc bias to the Gunn diode is provided directly to the center ring by a thin wire, which is not shown in the figure.

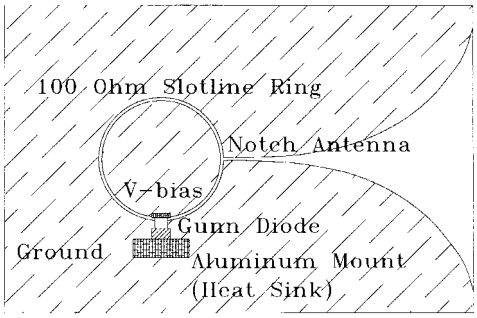

Fig. 2. Gunn-diode oscillator antenna configuration. The circuit does not have a metallized backplane. The slotline ring resonator has a mean radius of 3.88 mm and a gapwidth of 0.18 mm. The length of the antenna is 60 mm. The complete circuit was etched on a 78 mm × 38 mm piece of Duroid 5870 substrate, 1.575-mm-thick, 1-ounce copper metallization, and relative dielectric constant of 2.33. Note that some dimensions have been exaggerated to enhance detail, and the wire for dc bias to the center of the ring is not shown.

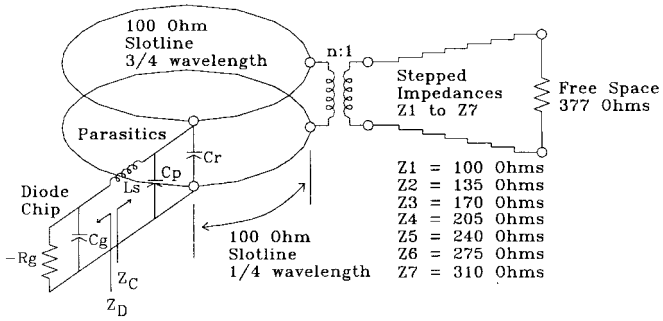

Fig. 3. Circuit model used for determining the frequency of oscillation. The Gunn diode used was an MA/Com 49 104-111, with $C_p = 0.27$ pF, $L_s = 0.30$ nH, $C_g = 1.05$ pF, and $R_g = 8\ \Omega$. The shunt capacitance C_r is approximately 1 pF. The transformer turns ratio is $n = 0.7$. The lengths of the antenna segments were set at 7.5 mm.

Determining the oscillating frequency of the circuit is straightforward. Using the circuit model shown in Fig. 3, the device and driving-point impedances can be found as functions of frequency. The Gunn diode used was an MA/Com MA 49104-111 rated for a minimum continuous wave (CW) power output of 25 mW. The diode package parasitics were provided by the manufacturer as typical values of $C_p = 0.27$ pF and $L_s = 0.30$ nH. The value of $C_g = 1.05$ pF is estimated from [10]. Since R_g is usually small, generally in the range of approximately 6–12 Ω [4], [6], [10]–[11], a value of 8 Ω is used as an approximation for the analysis of this experiment. The diode's negative resistance will decrease from $-8\ \Omega$ to $-8\ \Omega$ plus the residual resistance to a value of about $-3\ \Omega$ at the frequency of oscillation.

The parallel capacitance C_r is caused by the finite thickness of the metallization layer on the substrate and slotline gap. Using the parallel-plate approximation

$$C_r = \frac{2\pi r t \varepsilon_{\text{eff}}}{d} \tag{8}$$

where r is the radius of slotline ring, t is the metallization thickness, ε_{eff} is the effective dielectric constant, and d is the slotline gap. C_r can be found to be approximately 1 pF.

The discontinuity effects between the resonator ring and the slotline antenna are modeled as a transformer with a turn

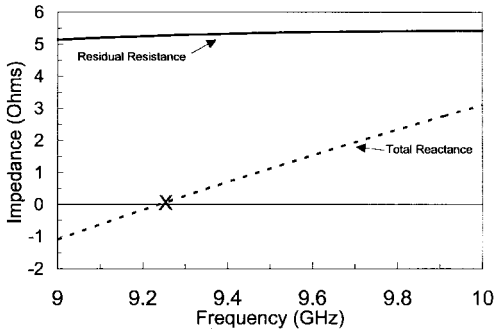

Fig. 4. Theoretical and experimental results of the frequency of oscillation. The "×" marks the measured oscillating frequency of 9.259 GHz for a Gunn-diode bias voltage of 10 dc voltage (VDC). The residual resistance must be greater than or equal to zero for oscillations to occur. The frequency of oscillation is the frequency at which the total reactance curve takes on a value of 0 Ω.

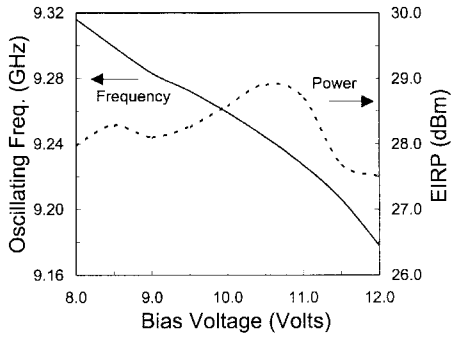

Fig. 5. Oscillator bias-tuning performance. The bias-tuning range is 138 MHz for Gunn-diode biases from 8 to 12 VDC. The output power is fairly constant for the tuning range, staying within 28 ± 1 dBm.

ratio $n:1$ with $n = 0.7$ obtained from the theory given in [12]. The slotline antenna was modeled as a seven-segment stepped-impedance transformer.

IV. Circuit Performance

From the model and the values given above, impedances Z_D and Z_C can be calculated, and the results plotted. Fig. 4 shows a plot of the "residual" resistance given by (3) and the total reactance. For the circuit to oscillate, the residual resistance must be greater than or equal to zero. The frequency of oscillation will be determined by the zero crossing of the total reactance curve. The large "×" shows the measured oscillation frequency at 9.259 GHz for a Gunn-diode bias voltage of 10 V. Considering that the modeling parameters are typical or calculated values, the experimental results show extremely good agreement with the model predictions.

Fig. 5 shows the bias-tuning performance of the oscillator antenna. The power output variations are within ±1 dB of +28-dBm effective isotropic radiated power (EIRP). The oscillator antenna provides a bias-tuning range of 138 MHz from 9.316 to 9.178 GHz for Gunn-diode biases from 8 to 12 V. The antenna radiated a clean spectrum with a phase noise of −95.33 dBc/Hz 100 kHz away from the carrier. The second harmonic produced is 26.16 dB below the fundamental frequency. This measured result is shown in Fig. 6.

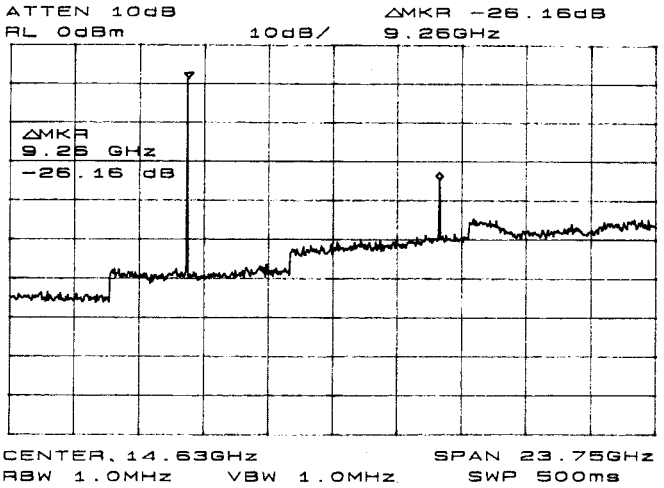

Fig. 6. Radiated spectrum. The second harmonic level is 26.16 dB below the fundamental frequency of 9.26 GHz.

The oscillator output is radiated by the slotline antenna. Fig. 7 shows the E- and H-planes radiation patterns of the oscillator antenna. The received power was measured in a mini-anaechoic chamber using Narda 640 standard horns at a distance of 1.2 m. The half-power beamwidths (HPBW's) are 33.0° and 47.0° for the E- and H-planes, respectively. Cross-polarization levels (CPL's) for the E- and H-planes were measured at 13.18 and 6.69 dB below co-polarization. These results compare well with those obtained from a similarly configured coplanar waveguide (CPW)-fed passive antenna. The passive antenna had HPBW's of 39.5° and 47.0° and CPL's of 18.74 and 16.51 dB below co-polarization for the E- and H-planes, respectively.

V. Varactor-Tunable Oscillator Antenna

The planar nature of the circuit allows for the easy integration of additional devices for increased functionality. Thus, a varactor diode was added to allow for wide-band tuning. These feature allows the circuit to be frequency modulated without much added complexity.

Fig. 8 shows the varactor-tunable oscillator antenna. The varactor used was an MA/Com MA 46600F-137 diode. Typical values for package parasitics were provided by the manufacturer as $C_v = 0.05$ pF and $L_v = 0.50$ nH. The other parameter values for the varactor diode were obtained from [6] and [10] as $R_s = 1\ \Omega$ and $R_j(v) > 10\ \text{M}\Omega$. The value of $C_j(v)$ is a function of the junction's reverse bias voltage v and is obtained from

$$C_j(v) = C_o\left(1 + \frac{v}{\phi}\right)^{-\gamma} \tag{9}$$

where C_o is the junction capacitance at zero bias, γ is a parameter that depends on the diode doping profile, and ϕ is called the built-in potential. The values given by the manufacturer were 1 pF, 0.5 ± 0.03, and 1.3 V, respectively.[1] The value for C_r decreases to 0.5 pF due to the additional bias

[1] M/A Com Semiconductor Products Operation, *M/A Com Semiconductor Products Catalog*, Burlington, MA, pp. 5.33–5.40 and A.17.

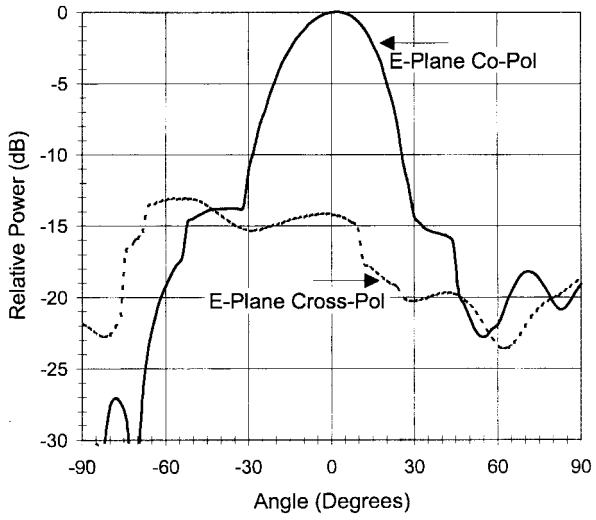

(a)

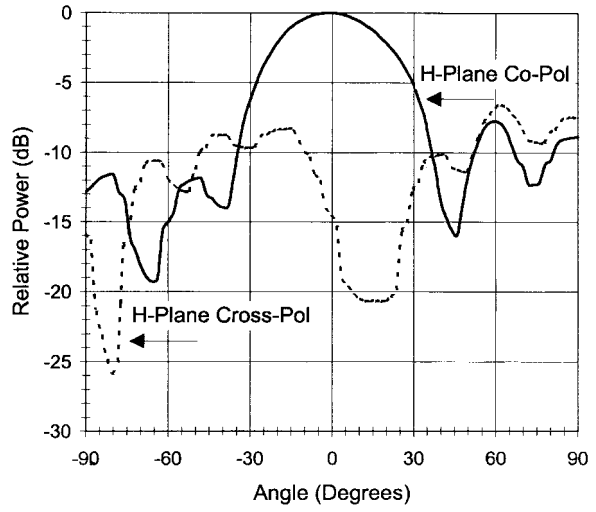

(b)

Fig. 7. (a) The E-plane radiation pattern shows an HPBW 33.0° and a CPL of 13.18 dB below co-polarization. (b) The H-plane radiation pattern shows a HPBW of 47.0° and CPL of 6.69 dB below co-polarization.

cut required for varactor biasing, which reduces the parallel-plate approximation area by one-half.

A simple model was developed to determine the frequency of operation and tuning range of the varactor-tuned oscillator antenna. Fig. 9 shows the transmission-line model. The experimental results agree extremely well with the model's prediction and are shown in Fig. 10, where the large "×s" mark the measured frequencies for varactor biases of 8 and 25 V, respectively. The measured frequencies agree very well with the zero crossings of the total reactance curves. There was a degradation of power output to 15 ± 3 dBm. A tuning range of nearly 400 MHz, or about 4%, was obtained. These measured results are shown in Fig. 11.

The radiation performance of the varactor-tunable antenna remained essentially unchanged throughout the tuning range. The phase noise was slightly improved to −103.2 dBc/Hz at 100 kHz away from the camera due to increased loaded Q of the circuit. However, the second harmonic level increased to 23.5 dB below the fundamental frequency.

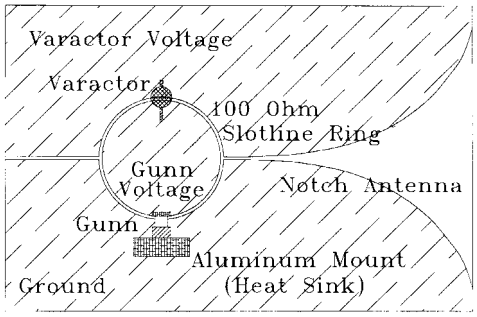

Fig. 8. The varactor-tuned oscillator antenna. The circuit does not have a metallized backplane. The slotline ring resonator has a mean radius of 3.88 mm and a gapwidth of 0.18 mm. The length of the antenna is 60 mm. The complete circuit was etched on a 78 mm × 38 mm piece of Duroid 5870 substrate, 1.575-mm-thick, 1-ounce copper metallization, and relative dielectric constant of 2.33. The additional dc cut is only about 0.8 mm. Note that some dimensions have been exaggerated to enhance detail, and the wires for dc biases are not shown.

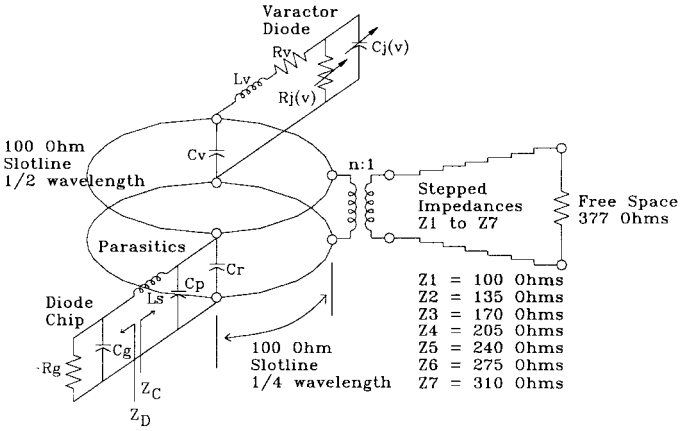

Fig. 9. Circuit model used for determining the frequency of oscillation. The varactor diode used was an MA/Com 49 600F-137, with $C_v = 0.05$ pF, $L_v = 0.50$ nH, $R_s = 1\ \Omega$, and $R_j(v) > 10\ \mathrm{M}\Omega$ in reverse bias. The shunt capacitance C_r is approximately 0.5 pF due to the additional bias cut needed for the varactor voltage. The transformer turns ratio is $n = 0.7$. The lengths of the antenna segments were set at 7.5 mm.

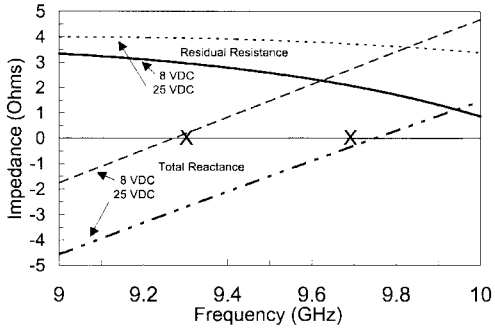

Fig. 10. Theoretical and experimental results for the varactor-tuned oscillator antenna. The "×" marks the measured oscillating frequencies of 9.308 and 9.691 GHz for varactor diode biases of 8 and 25 VDC, respectively.

VI. Self-Mixing and Injection-Locking Performance

Additional experiments were performed to study the self-mixing and injection-locking characteristics of the new configuration. In the self-mixing operation, the Gunn serves as a transmitter, local oscillator (LO), and mixer. The self-mixing

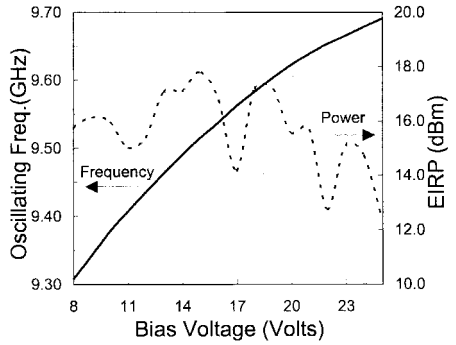

Fig. 11. Varactor tuning performance. The varactor tuning range is nearly 400 MHz for varactor voltages from 8 to 12 VDC. The output power has some variations for the tuning range, but it stayed within 15 ± 3 dBm.

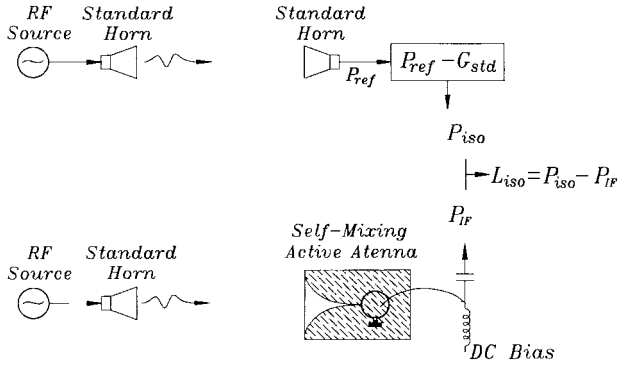

Fig. 12. Conversion-loss measurement setup. Narda 640 standard horns were used in the experiment. The power levels were measured with an HP8562A spectrum analyzer. A bias tee was used to prevent the intermediate frequency (IF) signal from leaking into the dc power supply.

performance of the oscillator active antenna was measured using the test setup shown in Fig. 12.

The distance separating the transmitting and receiving antennas was set to 1.58 m. The isotropic conversion loss is defined as the ratio of the isotropic received power to the IF power. Since isotropic radiators are unrealizable, Narda 640 standard horns with a gain of 16.3 dBi at 10 GHz were used to measure the reference power instead. $P_{\rm ref}$ was measured directly as -6.17 dBm. Thus, we obtain a $P_{\rm iso}$ of -22.47 dBm. The IF power was measured at -22.83 dBm, from which an isotropic conversion loss of 0.36 dB can be obtained. Since the slotline antenna gain was calculated to be 14.2 dB at 10 GHz, a double-sideband conversion loss of 14.56 dB or a single-sideband conversion loss of 11.56 dB is obtained.

The injection-locking test was performed using the setup shown in Fig. 13. When an external signal at frequency f_i with power P_i is directed at a free-running oscillator operating at frequency f_o with power output P_o, when f_i is close to f_o the free-running oscillator will injection-lock with the external signal and all the output power will be at frequency f_i. The ratio P_o/P_i is the locking gain, and the frequency difference between f_o and f_i is the one-side injection-locking bandwidth. The locking-gain versus locking-bandwidth results are shown in Fig. 14. A locking gain of 30 dB with a locking bandwidth of 17 MHz was obtained at 10 GHz. The Q-factor of the

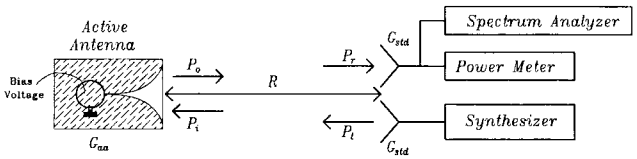

Fig. 13. Injection-locking test setup. The antennas used were Narda 640 standard horns. The spectrum analyzer was an HP8562A model. The power meter was an HP437B with an HP8481A power sensor. The synthesizer was an HP83622A sweeper.

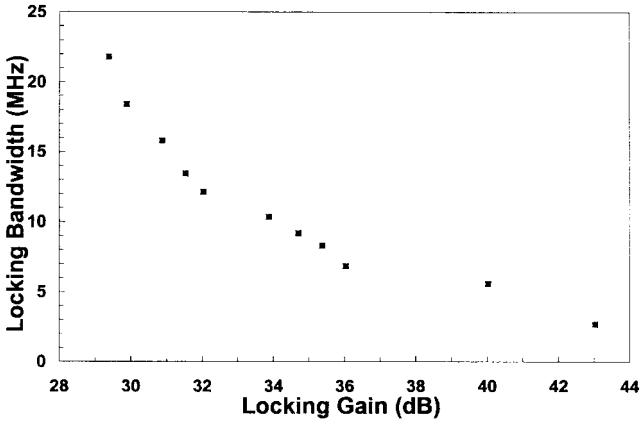

Fig. 14. Injection-locking performance. A locking-gain of 30 dB with a locking-bandwidth of 17 MHz was obtained at 10 GHz. An external Q-factor of 18.6 was computed using the above values.

antenna was calculated to be 18.6 using the equation found in [13]

$$Q_e = \left(\frac{f_o}{\Delta f}\right) \Big/ \left(\sqrt{\frac{P_o}{P_i}}\right) \tag{10}$$

where Q_e is the external Q-factor, f_o is the operating frequency, Δf is the one-side injection-locking bandwidth, P_o is the free-running oscillator power, and P_i is the injection-lock signal power.

VII. Conclusions

A Gunn diode has been integrated with a flared slotline antenna using a slotline ring resonator. The configuration was later modified to incorporate a varactor diode to form a varactor-tuned oscillator antenna. Simple models were developed to predict the circuits behavior. The models were validated by the experimental results obtained.

Both circuits exhibit good performance and offer a simple, rugged, lightweight, and low-cost tunable source for many microwave applications. Because the Gunn diode exhibits self-mixing performance, the device can be used as a half-duplex communications transceiver or as a Doppler radar frontend. If the self-mixing operation is not required, these oscillator antennas could be used in planar arrays for coherent spatial power combining due to their injection-locking characteristics, which could be accomplished through mutual coupling or with an external source.

REFERENCES

[1] W. K. Leverich, X. D. Wu, and K. Chang, "FET active slotline notch antennas for quasi-optical power combining," *IEEE Trans. Microwave Theory Tech.*, vol. 41, pp. 1515–1518, Sept. 1993.

[2] R. A. Flynt, L. Fan, J. A. Navarro, and K. Chang, "Low cost and compact active integrated antenna transceiver for system applications," *IEEE Trans. Microwave Theory Tech.*, vol. 44, pp. 1642–1649, Oct. 1996.

[3] Y. C. Yang, S. J. Chung, and K. Chang, "Active patch antennas integrated with FET's using coupled transmission lines," in *IEEE AP-S Int. Symp. Dig.*, vol. 1, Montéal, P.Q., Canada, July 1997, pp. 6–9.

[4] S. Nagano and Y. Akaiwa, "Behavior of Gunn diode oscillator with a moving reflector as a self-excited mixer and a load variation detector," *IEEE Trans. Microwave Theory Tech.*, vol. MTT-19, pp. 906–910, Dec. 1971.

[5] C. M. Montiel, L. Fan, and K. Chang, "A novel active antenna with self-mixing and wide-band varactor-tuning capabilities for communication and vehicle identification applications," *IEEE Trans. Microwave Theory Tech.*, vol. 44, pp. 2421–2430, Dec. 1996.

[6] K. Chang, *Microwave Solid-State Circuits and Applications*. New York: Wiley, 1994.

[7] S. Y. Liao, *Microwave Circuit Analysis and Amplifier Design*. Englewood Cliffs, NJ: Prentice-Hall, 1987.

[8] G. D. Vendelin, A. M. Pavio, and U. L. Rohde, *Microwave Circuit Design Using Linear and Nonlinear Techniques*. New York: Wiley, 1990.

[9] J. A. Navarro and K. Chang, "Varactor-tunable uniplanar ring resonators," *IEEE Trans. Microwave Theory Tech.*, vol. 41, pp. 760–766, May 1993.

[10] J. A. Navarro, Y. S. Shu, and K. Chang, "Broad-band electronically tunable planar active radiating elements and spatial power combiners using notch antennas," *IEEE Trans. Microwave Theory Tech.*, vol. 40, pp. 323–328, Feb. 1992.

[11] K. Chang, K. Louie, A. J. Grote, R. S. Tahim, M. J. Mlinar, G. M. Hayashibara, and C. Sun, "V-band low-noise integrated circuit receiver," *IEEE Trans. Microwave Theory Tech.*, vol. MTT-31, pp. 146–154, Feb. 1983.

[12] K. C. Gupta, R. Garg, and I. J. Bahl, *Microstrip Lines and Slotlines*, 2nd ed. Norwood, MA: Artech House, 1996, pp. 302–313.

[13] R. Adler, "A study of locking phenomena in oscillators," *Proc. IRE*, vol. 34, pp. 351–357, June 1946.

Claudio M. Montiel (S'91–M'93) was born in San Ramón, Costa Rica, in 1965. He received the B.S. degree from the University of Hawaii at Manoa, in 1988, the M.S. degree from Texas A&I University, Kingsville, in 1993, and the Ph.D. degree from Texas A&M University, College Station, in 1997, all in electrical engineering.

From 1988 to 1991, he was with the Western Geophysical Company of America, Houston, TX, where he worked with seismic data-acquisition crews for petroleum exploration in Gabon, Venezuela, and México. His duties included the operation, maintenance, and calibration of seismic data-recording equipment as well as helicopter time and recording crew management. He served as a Teaching Assistant at Texas A&M University for courses in "Ultra-High Frequency Techniques" and "Electrical Circuits and Instrumentation." He is currently with the Semiconductor Group, Texas Instruments Incorporated, Dallas, TX. His current research interests are in the areas of RF and microwave circuit design and metrology.

Dr. Montiel received The Regents' Fellowship and a U.S. Department of Education Fellowship for Research in Areas of National Need.

Lu Fan (M'96) received the B.S. degree in electrical engineering from the Nanjing Institute of Technology (now Southeast University), Nanjing, China, in 1982.

From September 1982 to December 1990, he was with the Department of Radio Engineering, Nanjing Institute of Technology, as a Teaching Assistant and Lecturer. In January 1991, he became a Research Associate in the Department of Electrical Engineering, Texas A&M University, College Station, TX. He is currently with Texas Instruments Incorporated, Dallas, TX. His interests include RF and microwave circuit design and testing.

Kai Chang (S'75–M'76–SM'85–F'91) received the B.S.E.E. degree from the National Taiwan University, Taipei, Taiwan, R.O.C, in 1970, the M.S. degree from the State University of New York at Stony Brook, in 1972, and the Ph.D. degree from the University of Michigan at Ann Arbor, in 1976.

From 1972 to 1976, he worked for the Microwave Solid-State Circuits Group, Cooley Electronics Laboratory, University of Michigan, as a Research Assistant. From 1976 to 1978, he was with Shared Applications, Inc., Ann Arbor, MI, where he worked in computer simulation of microwave circuits and microwave tubes. From 1978 to 1981, he was with the Electron Dynamics Division, Hughes Aircraft Company, Torrance, CA, where he was involved in the research and development of millimeter-wave solid-state devices and circuits, power combiners, oscillators and transmitters. From 1981 to 1985, he was with TRW Electronics and Defense, Redondo Beach, CA, as a Section Head, involved in developing state-of-the-art millimeter-wave integrated circuits and subsystems, including mixers, voltage-controlled oscillators (VCO's), transmitters, amplifiers, modulators, upconverters, switches, multipliers, receivers, and transceivers. In August 1995, he joined the Electrical Engineering Department, Texas A&M University, College Station, as an Associate Professor, and became a full Professor in 1988. In January 1990, he was appointed E-Systems Endowed Professor of electrical engineering. His current interests are in microwave and millimeter-wave devices and circuits, microwave integrated circuits, integrated antennas, wide-band and active antennas, phased arrays, microwave power transmission, and microwave optical interactions. He has authored and coauthored *Microwave Solid-State Circuits and Applications* (New York: Wiley, 1994), *Microwave Ring Circuits and Antennas* (New York: Wiley, 1996), and *Integrated Active Antennas and Spatial Power Combining* (New York: Wiley, 1996). He was the Editor of the four-volume *Handbook of Microwave and Optical Components* (New York: Wiley, 1989, 1990), "Microwave and Optical Technology Letters," and the Wiley Book Series in Microwave and Optical Engineering. He has published over 300 technical papers and several book chapters in the areas of microwave and millimeter-wave devices, circuits, and antennas.

Dr. Chang received the Special Achievement Award from TRW in 1984, the Halliburton Professor Award in 1988, the Distinguished Teaching Award in 1989, the Distinguished Research Award in 1992, and the TEES Fellow Award in 1996 from Texas A&M University.